SOLIDIFICATION OF AQUEOUS SOLUTIONS

by

David Nichols French

S.B., Massachusetts Institute of Technology, 1958

S.M., Massachusetts Institute of Technology, 1959

SUBMITTED IN PARTIAL FULFILLMENT OF THE

REQUIREMENTS FOR THE DEGREE OF

DOCTOR OF SCIENCE

at the

MASSACHUSETTS INSTITUTE OF TECHNOLOGY

May 1962

Signature of Author

Department of Metallurgy
May 1962

Thesis Supervisor

Professor C. M. Adams, Jr.

Chairman,
Department Committee
on Graduate Students

Professor J. T. Norton

SOLIDIFICATION OF AQUEOUS SOLUTIONS

by

David N. French

SUBMITTED TO THE DEPARTMENT OF METALLURGY
ON MAY 12, 1962, IN PARTIAL FULFILLMENT OF THE
REQUIREMENTS FOR THE DEGREE OF DOCTOR OF SCIENCE

ABSTRACT

A theoretical model for predicting the relationship between dendrite spacing and freezing time based on heat flow and mass transport considerations is presented. It is found theoretically and verified experimentally that the dendrite spacing is proportional to the degree of constitutional supercooling sustained in the interdendritic liquid and the square root of the solute diffusivity and the square root of the freezing time, and inversely proportional to the initial solute concentration and the slope of the liquidus curve of the phase diagram. The dendrite spacing increases with increasing values of diffusivity and, for potassium chloride, with increasing concentration. The amount of supercooling is calculated from the slope of the linear relationship between dendrite spacing and square root of freezing time. In all cases the amount of supercooling is less than 0.13°F and depends on the concentration and nature of the solute. The larger the solute diffusivity is, the smaller the degree of supercooling is.

A method for determining the thermal coefficients of a freezing medium, thermal conductivity, and heat transfer coefficient, is presented. The calculations are based on equating the quantity of heat liberated by a freezing sphere of ice to the amount of heat that crosses the ice-"mold" interface. By suitably handling the directly measurable variables, sphere diameter, and freezing time, the values of the thermal conductivity and heat transfer coefficient can be obtained from slopes and intercepts of straight lines. Using this technique, the thermal conductivity and heat transfer coefficient of an 80 per cent mineral oil - 20 per cent kerosene mixture were found to be 0.128 BTU/ft hr ^{o}F and 46.7 BTU/ft^2 hr ^{o}F, respectively.

Thesis Supervisor: Professor C. M. Adams, Jr.
Associate Professor of Metallurgy

TABLE OF CONTENTS

LIST OF ILLUSTRATIONS

LIST OF TABLES

ACKNOWLEDGMENTS

The author wishes to express his indebtedness to Professor Clyde M. Adams, Jr. for making graduate school possible and for his encouragement and technical guidance during the course of this study.

The author is also grateful to the Air Force Cambridge Research Laboratory, Terrestrial Sciences Laboratory, whose sponsorship also made this program possible.

He wishes further to thank the following people who have contributed to the success of the work: Mr. Russell E. Miller and other members of the Ice Laboratory staff who, from time to time, assisted with the experimental program; Miss Carolyn Ciccarelli, who offered to type this thesis; and all those with whom he discussed solidification.

Finally, the author wishes to thank his wife, whose understanding and tolerance created an atmosphere conducive to the completion of this study.

I. INTRODUCTION

The solidification of most aqueous salt solutions is accompanied by a complete unmixing of pure ice from the brine. As the temperature is decreased from the melting point, the ice that forms is not a solid solution of the salt in ice but the pure solvent. The fundamental behavior of solute atoms or ions and their mobility and rearrangement in the liquid during solidification can be more easily studied when the problem of handling the solute partition between liquid and solid at the interface is nonexistent. In this case, all solute must remain in the liquid until the eutectic temperature is reached and the salt precipitates as a hydrate.

There are some practical reasons why the phenomena of mass transport is important during solidification. For one thing, the movement of solute atoms away from the liquid-solid interface determines the freezing morphology of the solid and this in turn determines the crystal size. From the standpoint of desalination of sea water, the size of the ice crystals formed governs the efficiency of the purification process. For use in polar operations as a construction material, the strength properties of frozen sea water depend on the crystal size and brine distribution. In both instances the interplay of freezing rate and solute diffusion has the important role.

When pure water has its temperature lowered from, say 20°C, to its freezing point and then is frozen, several important changes

occur. The density increases with decreasing temperature until a maximum is reached at about $+4\,^{o}C$[1] and, on further cooling, decreases until ice begins to form at the freezing point. It is generally agreed that liquid water, at least below $+4^{o}C$, has a 4 coordinated crystalline-like structure, but unlike ice, the hydrogen bonds are continually being interchanged due to thermal fluctuations and the mobility of the molecules.[2] The tendency is for each water molecule to be surrounded in a tetrahedron fashion by four others. The structure of liquid water and ice has been compared with the quartz and tridymite forms of silica.[3] In both cases, the coordination number is 4, but the arrangement of the SiO_2 groups is somewhat different from the H_2O groups. It is considered that the quartz-like structure predominates in the liquid and this accounts for the increase in density on melting, for the quartz is a more closely packed structure than tridymite.

As solute is added to pure water, the maximum density and freezing point temperatures change. In sea waters of greater than 2.47 per cent total solute concentration, the freezing point is above the maximum density.[4] Presumably the addition of salts would have an influence on the "structure" of water.

On further cooling, under equilibrium conditions, ice begins to form promptly on reaching the freezing point. Once ice has nucleated, whether by using a favorable group of "structured" liquid molecules or by some foreign particle, or by the sides of the container, the further growth depends on the addition of individual liquid molecules, more or less randomly oriented, to the well ordered and oriented solid. Liquid

water may have a degree of long-range order; whether it does or not, the surface of a growing ice crystal can accept single liquid molecules only. If an ice crystal had to accept a group of molecules that had some long-range structure, the chance that the orientation of the liquid would agree with the solid would be slim. Thus, to accept an oriented group would call for reorientation prior to its addition to the growing solid. This orientation factor would lead to a lower freezing point than melting point, since no preferred orientation is necessary for melting. However, in the equilibrium case, both melting and freezing occur at the same temperature, allowing for a minute temperature difference to make the transformation go at a finite rate.

Once an ice crystal is formed, the question of how new layers are added becomes important. If a classical two-dimensional nucleus is assumed, the inescapable conclusion is that with the amount of supercooling present in the region immediately before the interface, some other mechanism must be operating. There is insufficient supercooling to form a two-dimensional nucleus. Two-dimensional nucleation is not necessary if the crystal surface has either a screw dislocation that prevents a plane of atoms from completing itself[5,6] or an atomically rough surface where single atoms may easily locate.[7] Whatever the mechanism, the problem of nucleating the additional solid layers becomes unimportant in determining the solidification rate and the amount of supercooling in a system where heat is being removed through the solid layer.

The amount of supercooling before a growing ice crystal seems

to be independent of solidification rate, but does depend on the composition and nature of the solute. The amount of supercooling, less than 1°F, is present as soon as the ice-liquid interface is established. For a given volume of a particular solution, the total amount of solute that must unmix from the ice is constant. As the freezing rate changes, the morphology of the interface between solid and liquid will change to accommodate the removal of solute to maintain a constant degree of supercooling.

Under exceptional conditions, liquid water can be supercooled in bulk to almost -40°F,[8] that is, 70°F of supercooling. Crystal growth from such a system does not follow the same rules of growth as does a crystal growing from its liquid with heat removal through the solid. In the latter case, the volumw of ice frozen is proportional to the amount of heat removed. In the former case, the volume of ice formed is proportional to the degree of bulk supercooling[9] and the rate, which can be extremely large, is then limited by the heat transfer from solid to liquid.

Growth of ice crystals from a solution can be a rapid process and is governed by the rate of heat removed. That is, the volume of ice formed is proportional to the amount of heat removed. The form of growth depends on the rate of growth because as more and more solid forms, the solute, which has no solubility in the solid, must re-distribute itself before the interface. This leads to a pile-up of solute at the interface, which means that liquid some distance away from the interface is more ready to freeze than the liquid at the

interface. The interface then develops protrusions or dendrites to reach out for this dilute liquid that is more ready to solidify. The solute-rich liquid then freezes between the dendrites. Most of the solid forms by the thickening of dendrites once the network is established at the initial breakdown of the plane interface.

The subject of the stability and the factors that control the stability of a plane liquid-solid interface, as well as the morphology of the interface, have received much study. Once the liquid-solid interface is established, there is a solute concentration gradient away from the boundary. Corresponding to this concentration gradient is a solidification temperature gradient; the high concentration material adjacent to the solid wants to solidify at a lower temperature than the dilute solution some distance into the liquid. Thus, if the actual temperature gradient in the liquid is able to solidify the solution of lower freezing point at the interface, the interface will remain plane. However, if the actual temperature gradient in the liquid is unable to freeze the material next to the interface, then the interface will be unstable and will reach out into the more dilute region.

Rutter and Chalmers[10] have shown that small amounts of impurity have a profound effect on the interfacial structure and lead to a non-uniform interface. Tiller and Rutter[11] found that under the most severe freezing conditions available with their apparatus, zone refined lead would not freeze with anything but a smooth liquid-solid interface. Hucke, et al[12] were able to maintain a plane interface in aluminum by supplying heat to the liquid to keep large temperature gradients across the liquid-solid boundary, but still solidify

at a finite rate. Harrison and Tiller[13] have studied the interfacial morphology in dilute aqueous solutions under slow growth rates and found that the aqueous solutions behave similarly to the metal systems.

However well the problem of interfacial stability is understood, only a little work has been done on the correlation of dendrite spacing. Bolling and Tiller[14] have presented a theoretical relationship for dendrite spacing in terms of growth velocity, diffusivity, entropy of fusion, temperature gradient at the interface, interfacial energy, and solute concentration, but the relationship agrees with experiment only in form and does not accurately predict dendrite spacing. Brown and Adams[15] present an analysis for dendrite spacing in aluminum-copper alloys in terms of solute concentration, phase diagram information, amount of supercooling in the liquid, diffusivity, and freezing time. The data fit the theory remarkably well.

Aside from the work of Harrison and Tiller, very little work has been done on aqueous solutions. Himes, et al[16] have studied solute distribution and crystal size of ice made from concentrated (3.5%) sodium chloride and sea water solutions, but make no attempt at theoretical analysis. This study will attempt to present a theoretical model and verify it experimentally.

II. THEORY

PART 1. MASS TRANSPORT.

Since the phase diagrams of all solutes investigated exhibit decreasing liquidus temperature with increasing solute concentration, solute will be rejected at the solid-liquid interface. There will, then, be a solute concentration gradient away from the interface. Corresponding to the solute gradient will be a liquidus temperature gradient. These effects are schematically represented in Figure 1. If the actual temperature gradient in the liquid is not greater than the slope of the liquidus temperature versus distance curve, there will be a zone of constitutional supercooling in the liquid, Figure 2a. The more usual case is shown in Figure 2b (somewhat exaggerated), where the actual temperature everywhere is slightly below the liquidus temperature.

As soon as the first solid layer has formed, there is a solute build-up at the interface. Solidification continues by protrusions of solid reaching out for the more dilute solution that is more ready to freeze. The solute is conenctrated between protrusions rather than swept ahead of the solid front. With no solid solubility of the salts studied, the solute concentration in the dendrite is always zero.

The size or spacing of the dendrites is determined by how far the interface advances into the liquid. For a given volume of solution, the amount of solute that must unmix from the solid is constant regardless of the solidification rate. An ideally slow rate would give the

the solute sufficient time to diffuse away from the interface, keeping it always planer. As the freezing rate increases, the same number of solute atoms or ions must be removed from the interface, but the time for liquid diffusion is considerably reduced. To accommodate the increased volume per unit time, the interface "solves" the diffusion problem by forming just the "right" number of dendrites per unit area.

Even though the overall interface moves into the liquid region essentially parallel to the heat flow direction, most of the ice forms by thickening of the dendrites perpendicular to the heat flow path. In sea ice, for example, the gross interface is relatively smooth, but the skeletal zone may extend for several inches up to the solidifying ice sheet. This zone is made up of dendrites separated by quite thick brine layers, so the zone itself has practically no strength.

For unidirectional solidification, any change in freezing rate should manifest itself in a change in dendrite spacing. In sea ice, although brine removal from the interface is aided by gravity convection of the more dense solution, increase in dendrite spacing is found as freezing rate decreases. Weeks [17] reports that ice made from sodium chloride solutions under simulated sea ice growth conditions exhibits an increase in dendrite spacing with increasing thickness of ice. Under this kind of growth, increasing ice thickness means decreasing freezing rate.

Once the network of dendrites has formed, the volume of space the growing dendrites will occupy is essentially equal to that of the

final dendrite. Since the dendrites grow as platelets, large in two dimensions compared with the third, the typical dimension is the thickness. If there is diffusion controlled mass transport in the liquid, the interdendritic liquid away from the growing dendrite will be lower in solute than the liquid at the interface because of solute accumulation. The high solute concentration at the interface will diffuse into the liquid away from the interface (see Figure 3).

The concentration of solute away from the interface is symmetrical about an axis along the center line of the growing platelet. For convenience's sake, only the portion from the center line to the mid-plane of the interdendritic pool is presented in Figure 3. The solute distribution in the liquid must conform to Fick's Second Law:

$$\frac{\partial C}{\partial \theta} = D' \frac{\partial^2 C}{\partial x^2} \qquad (1)$$

where: C = concentration, moles/liter

θ = time, seconds

D' = diffusivity, cm^2/sec

X = distance from the center line of the dendrite, cm.

A particular solution to Equation (1), in which C_S is an integration constant to be determined by the proper boundary conditions, is:[18]

$$\frac{C_S - C}{C_S - C_0} = \text{erf} \frac{X}{2\sqrt{D'\theta}} \qquad (2)$$

where: C = concentration at point X

C_o = initial concentration, equal to the concentration at the mid-point in the interdendritic pool

$\text{erf } X = \frac{2}{\sqrt{\pi}} \int_o^X e^{-Z^2} \, d Z$, a tabulated function

At the liquid-solid interface:

$$X = \epsilon \qquad C = C_i \tag{3}$$

and C_i is assumed to be constant. When conditions (3) are imposed on Equation (2), the left-hand side of the Equation (2) is seen to be constant, hence, so must the right-hand side. Equation (4) defines β, a constant.

$$\beta = \frac{\epsilon}{2\sqrt{D' \theta}} \tag{4}$$

$$C_S - C_o = \frac{C_i - C_o}{\text{erfc } \beta} \tag{5}$$

where: $\text{erfc } \beta = 1 - \text{erf } \beta$.

The rate at which solute ions are "manufactured" at the interface must be equal to the rate at which they are able to diffuse away.

$$C_i \frac{d \epsilon}{d \theta} = - D' \left(\frac{d C}{d X} \right)_{X = \epsilon} \tag{6}$$

Differentiating Equation (2) and combining with Equations (5) and (6):

$$\frac{C_i - C_o}{C_i} = \sqrt{\pi} \, \beta \, e^{\beta^2} \, \text{erfc } \beta \tag{7}$$

The procedure outlined above consists of assuming the form of the solution, imposing the boundary conditions, and determining whether the boundary conditions are consistent with the assumed form. Since Equation (7) may be solved for a real value of β and all the necessary conditions are fulfilled, Equations (7), (2), and (6) are the solution.

If: $\beta < 0.05$ (8)

then: $e^{\beta^2} \operatorname{erfc} \beta \approx 1$ (9)

and: $$\sqrt{\pi}\beta \approx \frac{C_i - C_0}{C_i} \approx \frac{\Delta T}{m C_0} \quad (10)$$

where: m = slope of liquidus line on the phase diagram, ^{o}F/moles/liter

ΔT = amount of supercooling, ^{o}F

From Equation (4):

$$\epsilon_f = 2 \beta \sqrt{D' \theta_f} \quad (11)$$

where: ϵ_f = final half thickness of the dendrite

θ_f = freezing time

Combining Equations (10) and (11) and noting that $\epsilon_f = \frac{L}{2}$:

$$L = \frac{4 \Delta T \sqrt{D' \theta_f}}{\sqrt{\pi}\, m C_0} \quad (12)$$

It should be noted that if during solidification any changes in D', ΔT, m, and C_0 occur, this may cause the plane interface of the dendrite to become unstable and cause secondary dendrites. The

secondary dendrites will have a new and smaller value of L. If, however, the changes in D', ΔT, m, and C_0 predict a greater spacing than is established, the existing spacing is stable and will not be altered.

PART 2. HEAT FLOW.

Consider an infinite medium of initial temperature, T_0 °F, surrounding an internal spherical cavity of diameter, D, inches. At zero time, the temperature of the cavity is raised to a constant temperature, T_M. Assume the interface has a constant temperature, T_S. T_S may be thought of as a time averaged value. The amount of heat, Q BTU, that enters the medium is:[19]

$$Q = A K (T_S - T_0) \left(\frac{2 \theta_f}{D} + \frac{2\sqrt{\theta_f}}{\sqrt{\pi \alpha}} \right) \qquad (13)$$

where: A = cavity area, in^2

K = thermal conductivity of the medium, BTU/in min °F

θ_f = time, min

$\alpha = K/\rho' C_P$ = thermal diffusivity, in^2/min

C_P = heat capacity of the medium, BTU/lb °F

The same quantity of heat must have crossed the boundary surface of the cavity and is given by:[19]

$$Q = A h (T_M - T_S) \theta_f \qquad (14)$$

where: h = coefficient of heat transfer, BTU/in^2 min °F

Equations (13) and (14) may be combined to eliminate the unknown interface temperature, T_S:

$$\frac{A}{Q}(T_M - T_O) = \frac{1}{h\,\theta_f} + \frac{1}{\frac{2K\theta_f}{D} + \frac{2K\sqrt{\theta_f}}{\sqrt{\pi\alpha}}} \tag{15}$$

If the cavity is water at its freezing point, Q is then:

$$Q = V \rho H \tag{16}$$

where: V = cavity volume, in^3

ρ = water density, 0.036 lbs/in^3

H = heat of fusion of water, 142 BTU/lb

For a sphere:

$$\frac{V}{A} = \frac{D}{6} \tag{17}$$

where: D = diameter, in.

Combining Equations (15), (16), and (17):

$$\frac{\theta_f}{D} = \frac{\rho H}{6(T_M - T_O)h} + \frac{\rho H}{12(T_M - T_O)K}\left[\frac{1}{\frac{1}{D} + \frac{1}{\sqrt{\pi\alpha\theta_f}}}\right] \tag{18}$$

Let:
$$Z = \frac{\rho H}{6(T_M - T_O)h} \tag{19}$$

and:
$$Y = \frac{\rho H}{12(T_M - T_O)K} \tag{20}$$

From Equation (18), using (19) and (20), a quadratic equation in D may be found:

$$D^2 \left(Z + Y\sqrt{\pi\alpha\theta_f}\right) + D\left(Z\sqrt{\pi\alpha\theta_f} - \theta_f\right) - \theta_f\sqrt{\pi\alpha\theta_f} = 0 \qquad (21)$$

Solving for D:

$$D = \frac{\left(\theta_f - Z\sqrt{\pi\alpha\theta_f}\right) + \left[\left(Z\sqrt{\pi\alpha\theta_f} - \theta_f\right)^2 + 4Z\theta_f\sqrt{\pi\alpha\theta_f} + 4Y\pi\alpha\theta_f^2\right]^{1/2}}{2Z + 2Y\sqrt{\pi\alpha\theta_f}} \qquad (22)$$

Equation (22) may be simplified for values of θ_f greater than about four minutes. Under these conditions, Z may be neglected compared with $Y\sqrt{\pi\alpha\theta_f}$, $Z\sqrt{\pi\alpha\theta_f}$ may be neglected compared with θ_f, and only the θ_f^2 terms inside the brackets are of significance.

$$D \approx \frac{\theta_f^{1/2}\left\{1 + \left[1 + 4Y\pi\alpha\right]^{1/2}\right\}}{2Y\sqrt{\pi\alpha}} \qquad (23)$$

A plot of D versus $\theta_f^{1/2}$ will be linear, see Figure 4, and the slope of the data found by the method of least squares will be:

$$\text{Slope} = \frac{\left\{1 + \left[1 + 4\pi Y\alpha\right]^{1/2}\right\}}{2Y\sqrt{\pi\alpha}} \qquad (24)$$

From Equation (24), a reasonably accurate value of K may be determined.

A plot of Equation (18):

$$\frac{\theta_f}{D} \quad \text{versus} \quad \frac{1}{\frac{1}{D} + \frac{1}{\sqrt{\pi\alpha\theta_f}}}$$

should be a linear function with slope proportional to 1/K and intercept proportional to 1/h. A comparison of Figures 4 and 5 shows that

there is a great deal more scatter in Figure 5 (Equation (18)) than in Figure 4 (Equation (23)). In Figure 4, the slope is a function of K, and K is expected to be insensitive to minor variations in the medium. The intercept value of Figure 5 is dependent on h, and h is quite sensitive to small variations in the interface configuration, hence, more scatter in Figure 5.

Some feel for the magnitude of h can be had by using the intercept of Equation (18) found in the following manner. From Equation (24) a reasonably accurate value of K may be determined. The slope of Equation (18) may then be computed, using this value of K. Next, the "center of mass" of the data in Figure 5 is calculated, and this point plus the known slope of the line will give the intercept. The curve in Figure 5 is given a slope corresponding to the K value of Equation (24), and is forced to pass through the "center of mass" of the data. The limits of h are found by calculating the standard deviation of the data from the line used to find h and using the 95 per cent confidence limits, that is, two standard deviations on either side of the intercept.

The curved tail portion of Figure 4 for θ_f less than about four minutes is computed from Equation (22), using the experimental values of K and h. For θ_f greater than four minutes, the two curves are almost coincidental.

III. EXPERIMENTAL PROCEDURE

The experimental portion of the study was divided into two main areas: (a) the measurement of the solidification time of various size ice spheres, and (b) the measurement of dendrite spacing. An empirical relationship that agrees in form to that expected theoretically was developed between a size parameter and freezing time. Thus, in correlating dendrite spacing with freezing time, by measuring the size of a particular sphere the freezing time was effectively determined.

A. Freezing Time Measurements.

The "mold" into which the ice spheres were "cast" was a beaker of organic liquid at $-4^{\circ}F$. A mixture of 20 per cent kerosene and 80 per cent mineral oil was chosen for its clarity, insolubility in water and water in it, and high viscosity. It was necessary to use a clear fluid so that the thermocouple junction could be easily seen to facilitate centering the sphere at the junction. A liquid that is neither dissolved by nor dissolves water was required; otherwise, the sphere would disappear or change composition and thus its freezing point. Since it was impossible to find a non-toxic liquid that has a density close to that of water or ice, the next best thing was to use a liquid of high viscosity to prevent the sphere from either floating or sinking too rapidly during the temperature measurements. The surface tension of the solutions used tended to make the drop spherical, but the density difference between "mold" and solution caused the spheres to be slightly elliptical.

For all temperature measurements, copper-constantan thermocouples were used and temperature was continuously recorded on a single-channel Brown instrument. Two thermocouple wire sizes were used, 4 and 20 mil, to study the influence of the wire size on the freezing time. The 4-mil wire was welded with a gas torch, and the 20-mil wire butt welded with a capacitor discharge welder. In both cases the thermocouple was used in the straight position with the junction in the center of the beaker.

B. Solution Preparation.

Four solutes were investigated for their wide variation in diffusivity values, greater than a factor of three, and similar phase diagrams, i.e. sodium chloride, potassium chloride, lithium chloride, and hydrochloric acid (see Table I). Potassium chloride was investigated in several compositions from about 0.2 to 0.6 moles per liter.

In all cases the solutions were prepared in the same fashion. Demineralized water was boiled for at least ten minutes to exclude any dissolved gases and stored, while cooling, in a closed container. The solutes were weighed on a triple-beam balance to yield the proper solute concentrations and then checked by titration. Potassium chloride, sodium chloride, and lithium chloride were analyzed by the method of Mohr,[23] using standardized silver nitrate solution and titrated to a potassium chromate end point. Hydrochloric acid was titrated to a phenothalein end point with standardized sodium hydroxide solution.

TABLE I

Phase Diagram Information, Diffusivities, and Solute Concentrations of Solutions Investigated

Salt	Concentration moles/liter	Slope of Liquidus[20] °F/mole	Diffusion Coefficient[21,22] (Corrected to Freezing Point)	Eutectic Temperature °F
KCl	0.204	-5.85	0.81×10^{-5}	+12
	0.299	-5.85	0.81×10^{-5}	
	0.364	-5.85	0.80×10^{-5}	
	0.405	-5.85	0.80×10^{-5}	
	0.603	-5.85	0.78×10^{-5}	
HCl	0.395	-6.62	1.60×10^{-5}	-120
LiCl	0.401	-6.32	0.47×10^{-5}	below -6
NaCl	0.403	-6.08	0.62×10^{-5}	-6

After analysis, 10 or 12 drops of vegetable dye were added to each 200 milliliter solution. The dye aided in the observation of the dendrite spacing. The colored solution was then cooled to its freezing point by noting when the first ice formed. The solution was used for either dendrite spacing or freezing time determinations.

C. Dendrite Spacing Measurements.

Spheres were made in a 30-inch tall by 3 inch in diameter column filled with the 20 per cent kerosene and 80 per cent mineral oil mixture and maintained at -4°F. The size range of the spheres that were made ranged from about 0.1 inch to 0.5 inch in diameter. The spheres were removed from the column by a wire basket. After solidification, the spheres were measured with a micrometer in several places and the smallest measurement used as the diameter. With a micrometer, three significant figures could easily be obtained.

After measurement the spheres were mounted in grease for polishing and photographing. The samples were polished on normal metallographic polishing paper and smoothed up to final polish on a paper towel. Following this treatment, the samples were photographed at about seventy magnification. At least two photographs of separate regions were made. To correct for any difference in magnification due to changes in film or processing from roll to roll, each set of samples, that is, one roll of 36 exposures of 35 millimeter film, included a photograph of a 1 millimeter grid. The magnification of the set was determined from the grid photograph.

The measurements of dendrite spacing were made from the photographs. Each dendrite measured had several values of its width made and each sphere had at least 20 dendrites measured. Since the observed dendrite spacing is not the minimum or actual spacing, one drop was photographed 34 times to develop a more complete distribution. Figure 8 gives the frequency versus observed spacing for 200 observations.

IV. RESULTS

Since the measurement of solidification time depends on an accurate "end point" to the freezing process, and all the solutions investigated freeze over a range of temperatures, there is no sharp break at an "end point" in the time-temperature graphs recorded. Only a gradual decrease in temperature is observed (see Figure 6). Therefore, the "end point" is arbitrarily taken as $3^{o}C$ below the initial freezing point. It is assumed that there is a unique relationship between the time it takes for the temperature to fall $3^{o}C$ and the freezing time. It should be pointed out, however, that with all the solutions used, the eutectic temperature, and thus the temperature for complete solidification, is well below $-3^{o}C$ (see Table I). The dendrite spacing is established early in the freezing process and the time for the temperature to fall $3^{o}C$ is sufficient to satisfy the freezing time.

The results of the freezing time measurements are presented in Figures 4 and 5. No significant difference is observed in the freezing times as measured by the two thermocouple wire sizes used (4 and 20 mil). These data are treated together. A least squares analysis of Figure 4 for the best straight line gives:

$$D = 0.173\ \theta_f^{1/2} - 0.079 \qquad (25)$$

Using Equation (24) with the slope of 0.173 from Equation (25) gives:

$$0.173 = \frac{\left\{1 + \left[1 + 4\pi Y \alpha\right]^{1/2}\right\}}{2 Y \sqrt{\pi \alpha}} \qquad (26)$$

Noting that:

$$\alpha = \frac{K}{\rho' C_p} \qquad (27)$$

Equation (26) may be solved for K, the thermal conductivity of the medium. Using $\rho' = 0.033$ lb/in^3, a measured quantity, $C_p = 0.5$ BTU/lb ^oF, a handbook value for oils of this nature, $Y = \frac{0.0118}{K}$, from its definition and the constants given before with $T_M - T_0 = 36^oF$, K is found to have a value of 0.128 BTU/ft hr ^oF.

Using the method outlined in Section II, the equation of the line through the "center of mass" of the data in Figure 5 with the slope proportional to the reciprocal of the K value found above is:

$$\frac{\theta_f}{D} = 4.37 + \frac{66.5}{\frac{1}{D} + \frac{1}{\sqrt{\pi \alpha \theta_f}}} \qquad (28)$$

with a standard deviation in θ_f/D of 1.06. From the intercept value of 4.37, the value of h is 46.7 BTU/ft^2 hr ^oF. Taking the error in h to be twice the standard deviation on either side of 4.57, h varies from 32.0 to 92.0 BTU/ft^2 hr ^oF.

To establish the final shape of the ice dendrites, a single sphere of 0.405 mole/liter KCl solution was frozen in the usual fashion. Two facets were polished at 90^o to each other and photographed close to the apex of the included right angle. The apex was then polished flat at 45^o to each of the original facets for a depth of about a millimeter,

giving a flat surface of about twice that size. This area, which encompassed the same dendrites as the previous pictures, was also photographed. Figure 7 shows the three regions. Figure 7a is 90° to Figure 7c, and Figure 7b is 45° to each of the other two. There can be little doubt that the dendrites of ice grow as platelets, long in two dimensions and short in the third.

The relationship between the observed dendrite spacing, L, for a given freezing time and the true or actual dendrite spacing, L_0, is:

$$\sin \gamma = \frac{L_0}{L} \tag{29}$$

where γ is the angle between the plane of the dendrite and the observed surface. The angle, γ, may have any value from 90°, corresponding to an observation of the true dendrite spacing, to almost zero. If the smallest value of L observed is assumed to be L_0, the average value of γ is:

$$\bar{\gamma} = \sin^{-1} \frac{L_0}{L_{Ave.}} \tag{30}$$

From the distribution of the observed L (Figure 8), the smallest L is 0.0040 cm. and the average is 0.00696 cm., thus:

$$\bar{\gamma} = \sin^{-1} \frac{0.0040}{0.00696} \approx 35^\circ \tag{31}$$

However, knowing L_0, an average γ from the distribution may be calculated by computing for each observation the corresponding γ and summing over the entire distribution. This average, γ', is

approximately 38°, that is:

$$\sin \gamma' = 0.614 \approx 38^{\circ}$$
$$\sin \bar{\gamma} = 0.575 \approx 35^{\circ} \qquad (32)$$

The agreement between the two averages is quite good considering that the value of L can be measured only to 0.0005 cm. The value of $\sin \bar{\gamma} = 0.575$ was used to correct the average L to L_0.

Figure 8 is the distribution of observed dendrite spacing for 200 observations. The average of the distribution is 0.00696 cm.; the averages of the first and second groups of 20 observations are 0.00704 cm. and 0.00693 cm., respectively. It is assumed that an average of at least 20 observations does not significantly differ from the actual average.

The necessary constants of the salts used are summarized in Table I, and the phase diagrams for the region of interest are presented in Figure 9. The diffusion coefficients are taken from Electrolyte Solutions[21] and corrected to the freezing points by the method given by Newman,[22] (see Appendix 5). There is no appreciable difference in the phase diagrams of the salts investigated. The only difference is in the value of the diffusion coefficients, which vary by a factor of about three.

The analysis presented in Section II predicts a linear relationship between dendrite spacing and the square root of freezing time. Figures 10 and 11 show that this is the case for the solutes investigated. Figure 10 shows that as the solute concentration increases

so does the dendrite spacing and slope of the line, which means that the amount of supercooling increases. Figure 11 shows that for a constant composition, the dendrite spacing increases with an increase in the diffusion coefficient. Quantitative analysis of the slopes, found by the method of least squares, leads to a value for the amount of constitutional supercooling sustained by the interdendritic liquid. In Figure 12 the terms $\Delta T\sqrt{D'}$ are plotted versus the concentration for the KCl solutions. Table II summarizes these results. In general, the amount of supercooling increases with decreasing diffusion coefficient for a constant or nearly constant composition and increasing concentration for a single solute.

When the curves in Figures 10 and 11 are extrapolated to zero time, a finite dendrite spacing is predicted for an infinite freezing rate. This appears to be at odds with the theory. The discrepancy may be explained, at least in part, by noting that the curve of the diameter versus the square root of freezing time (Figure 4) extrapolates to a finite time to freeze a zero diameter sphere. A graph of diameter versus dendrite spacing would also miss the origin in the same way; a zero diameter sphere would have a finite dendrite spacing. By shifting the origin in Figure 4 to extrapolate linearly to the origin would bring the curves in Figures 10 and 11 more nearly to the origin. In this event, the slope would not be altered and the important quantity, ΔT, would not be affected.

TABLE II

Supercooling Calculated from Equation (12)

Salt	Concentration moles/liter	$-\Delta T$ °F	$\frac{\Delta T \sqrt{D'}}{^{\circ}F \text{ cm/sec}^{1/2}}$
KCl	0.204	0.025	7.09×10^{-5}
	0.299	0.047	13.3×10^{-5}
	0.364	0.065	18.4×10^{-5}
	0.405	0.066	18.7×10^{-5}
	0.603	0.123	34.4×10^{-5}
HCl	0.395	0.066	26.5×10^{-5}
LiCl	0.401	0.090	19.5×10^{-5}
NaCl	0.403	0.075	18.7×10^{-5}

Figure 13 is a comparison of the dendrite spacing for a constant composition but widely different freezing times; as expected, the slower the freezing rate, the wider the dendrite spacing. In Figure 14, the effect of increasing the diffusion coefficient on dendrite spacing is shown for essentially constant freezing time and composition. Again, an increase in the value of D' causes an increase in the dendrite spacing. Figure 15 shows the effect of increasing the concentration of potassium chloride on dendrite spacing while maintaining a constant freezing time.

V. CONCLUSIONS

1. The linear relationship between dendrite spacing and the square root of the freezing time predicted by the theoretical solidification model has been verified experimentally.

2. Dendrite spacing increases with solute concentration for potassium chloride.

3. Interpretation of the data strongly indicates that dendrite spacing increases with an increasing value of the solute diffusivity for a constant solute concentration.

4. When the experimental data are fitted to the proposed solidification model, the amount of constitutional supercooling within the interdendritic liquid, as calculated from the theory, is quite small, less than $0.13^{\circ}F$, and depends on the amount and nature of the solute. For potassium chloride solutions, the amount of supercooling increases with increasing concentration. The amount of supercooling decreases as the value of the diffusion coefficient increases.

5. The measurement of freezing times for a size range of spheres can be used to determine the thermal constants of the freezing

medium. In this manner, the thermal conductivity of the medium was found to be 0.128 BTU/ft hr ^{o}F, and the heat transfer coefficient 46.7 BTU/ft^{2} hr ^{o}F.

VI. SUGGESTIONS FOR FUTURE WORK

1. Fundamental information correlating dendrite size and freezing time should be obtained for sea water and other impure waters used in desalination processes. It is of prime importance in the effective use of freezing as a means of manufacturing potable water that this kind of information be available.

2. It would be of scientific interest to use a solute, ammonium fluoride for example, which exhibits some solid solubility in ice.

APPENDIX 1

List of Symbols Used

A = area of sphere, in^2

C = solute concentration, moles/liter

C_i = solute concentration at liquid-solid interface, moles/liter

C_o = initial solute concentration, moles/liter

C_p = heat capacity of freezing medium, 0.50 BTU/lb

C_s = integration constant in Equation (2)

D = diameter of sphere

D' = diffusivity of solute, cm^2/sec

H = heat of fusion of ice, 142 BTU/lb

h = heat transfer coefficient, BTU/ft^2 hr ^oF

K = thermal conductivity of the freezing medium, BTU/ft hr ^oF

L = observed dendrite spacing, cm

L_o = actual dendrite spacing, cm

m = slope of the liquidus line on the phase diagram, ^oF/mole

Q = amount of heat, BTU

T = temperature, ^oF

T_o = temperature of freezing medium, ^oF

T_M = melting point of ice, 32^oF

T_S = interface temperature, ^oF

ΔT = amount of supercooling, ^oF

V = volume of sphere, in^3

X = distance from centerline of dendrite, cm

$Y = \frac{\rho H}{12 (T_M - T_O) K}$, slope of Equation (18)

$Z = \frac{\rho H}{6 (T_M - T_O) h}$, intercept of Equation (18)

$\alpha = \frac{K}{\rho' C_P}$, thermal diffusivity, ft^2/hr (in^2/min)

β = a constant defined as $\frac{\epsilon}{2\sqrt{D' \theta}}$

γ = angle between plane of dendrite and observed sample surface

$\bar{\gamma}$ = average of $\gamma = \sin^{-1} \frac{L_O}{L_{Ave}}$

γ' = average of γ from distribution of observed dendrite spacing

ϵ = half thickness of dendrite, cm

ρ = density of water, 0.036 lbs/in^3

ρ' = density of freezing medium, 0.033 lbs/in^3

θ = time, seconds

θ_f = freezing time, min

APPENDIX 2

Freezing Time Measurements

4-mil thermocouple wire

D (in)	$\theta_f^{1/2}$ (min)	D (in)	$\theta_f^{1/2}$ (min)
0.320	2.41	0.307	2.24
0.382	2.54	0.257	2.01
0.433	2.92	0.338	2.30
0.238	1.84	0.342	2.48
0.275	1.97	0.491	3.26
0.389	2.68	0.337	2.50
0.242	1.93	0.312	2.45
0.412	2.87	0.235	2.00
0.359	2.59	0.271	2.03
0.232	1.68	0.372	2.66
0.382	2.62	0.305	2.25
0.294	2.17	0.326	2.30
0.236	1.77	0.412	2.87
0.317	2.29	0.269	1.88
0.412	2.79	0.229	1.82
20-mil thermocouple wire			
0.414	2.78	0.278	2.06
0.377	2.58	0.442	2.83
0.457	3.20	0.318	2.27
0.447	2.94	0.450	2.94
0.321	2.27	0.475	3.24
0.432	2.91	0.424	2.78
0.398	2.65	0.481	3.38

APPENDIX 3

Dendrite Spacing Measurements

KCl--0.204 moles/liter

D (in)	L_0 (cm) $\times 10^3$	$\theta_f^{1/2}$ (min)
0.313	3.13	2.27
0.399	3.89	2.76
0.270	2.78	2.02
0.384	3.36	2.68
0.231	2.55	1.79
0.480	4.18	3.23
0.164	2.09	1.40
0.126	2.09	1.22

KCl--0.299 moles/liter

0.513	5.57	3.42
0.445	5.34	3.03
0.437	5.57	2.98
0.334	4.64	2.39
0.241	3.94	1.85
0.161	3.19	1.39
0.143	2.96	1.23
0.265	3.83	1.99

D (in)	L_o (cm) $\times 10^3$	$\theta_f^{1/2}$ (min)
KCl--0.364 moles/liter		
0.481	6.26	3.18
0.355	5.57	2.51
0.147	3.54	1.25
0.275	4.70	2.05
0.546	7.19	3.61
0.409	5.57	2.82
0.211	4.00	1.68
KCl--0.405 moles/liter		
0.411	5.80	2.77
0.141	3.63	1.21
0.348	5.05	2.47
0.215	3.89	1.70
0.293	4.93	2.15
0.498	6.38	3.34
KCl--0.603 moles/liter		
0.541	9.16	3.58
0.333	6.26	2.38
0.233	5.28	1.80
0.390	6.73	2.71
0.140	4.40	1.21
0.304	5.80	2.21
0.460	7.19	3.12
0.104	4.47	0.98

D (in)	L_o (cm) $\times 10^3$	$\theta_f^{1/2}$ (min)
HCl--0.395 moles/liter		
0.473	9.16	3.19
0.444	8.18	3.02
0.361	7.54	2.54
0.248	6.61	1.89
0.158	5.34	1.37
0.139	5.45	1.20
0.440	8.35	3.00
LiCl--0.401 moles/liter		
0.455	5.45	3.09
0.370	5.00	2.60
0.293	4.12	2.15
0.209	3.60	1.66
NaCl--0.403 moles/liter		
0.468	6.03	3.16
0.490	5.86	3.29
0.356	4.99	2.51
0.309	4.70	2.82
0.224	3.94	1.81
0.232	3.89	1.80

APPENDIX 4

Calculations to Show that β is Less Than 0.05

If $\beta < 0.05$, then $e^{\beta^2} \operatorname{erfc} \beta \approx 1$.

$$\beta = \frac{\epsilon}{2\sqrt{D'\theta}} = \frac{L_o}{4\sqrt{D'\theta_f}}$$

$L_o/\theta_f^{1/2}$ is the slope of the L versus $\theta_f^{1/2}$ plots.

Salt	Concentration Moles/liter	$\frac{L_o/\theta_f^{1/2}}{cm/min^{1/2}}$	$\frac{\sqrt{D'}}{cm/min^{1/2}}$	β
KCl	0.204	1.10×10^{-3}	2.20×10^{-2}	0.0125
	0.299	1.44×10^{-3}	2.20×10^{-2}	0.0163
	0.364	1.52×10^{-3}	2.19×10^{-2}	0.0172
	0.405	1.38×10^{-3}	2.19×10^{-2}	0.0156
	0.603	1.70×10^{-3}	2.16×10^{-2}	0.0196
HCl	0.395	1.76×10^{-3}	3.10×10^{-2}	0.0139
LiCl	0.401	1.35×10^{-3}	1.68×10^{-2}	0.0193
NaCl	0.403	1.33×10^{-3}	1.93×10^{-2}	0.0172

APPENDIX 5

Temperature Correction for Diffusivity

Newman[22] gives the following equation for the temperature dependence of diffusivity:

$$D'_T = D'_{298}\left[1 + a\,(T - 298) + b\,(T - 298)^2\right]\frac{T}{298}$$

where: T is the absolute temperature.

Salt	a	b	Concentration	D' (298)[21]
KCl	$+2.17 \times 10^{-2}$	$+ 6.7 \times 10^{-5}$	.2	1.84×10^{-5}
			.4	1.84×10^{-5}
			.6	1.85×10^{-5}
HCl	$+1.63 \times 10^{-2}$	-1.6×10^{-5}	.4	3.14×10^{-5}
LiCl	$+2.65 \times 10^{-2}$	$+14.8 \times 10^{-5}$	.4	1.26×10^{-5}
NaCl	$+2.26 \times 10^{-2}$	$+ 8.4 \times 10^{-5}$	.4	1.47×10^{-5}

Figure 1

Relations Among Solute Concentration, Distance from a Freezing Interface, and Liquidus Temperature.

a. Temperature versus Solute Concentration.

b. Solute Concentration versus Distance.

c. Liquidus Temperature versus Distance.

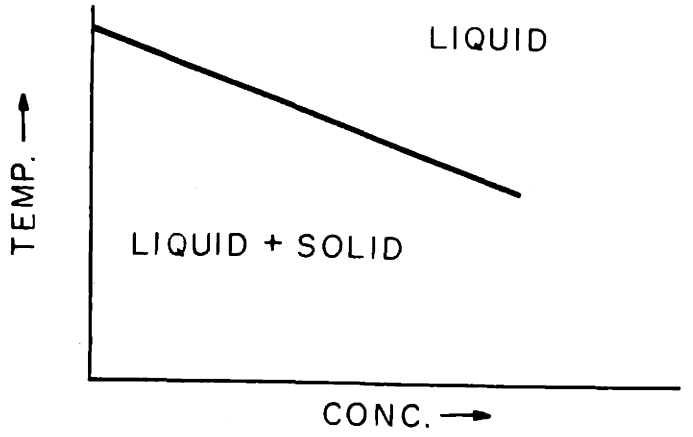
LIQUID
TEMP.
LIQUID + SOLID
CONC.

A

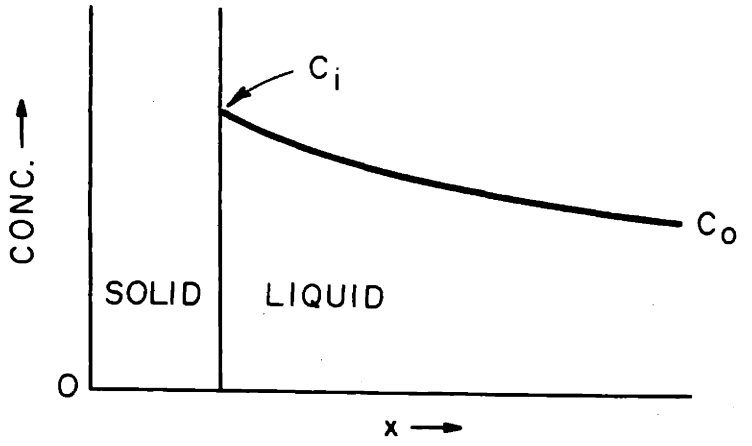
C_i
CONC.
C_o
SOLID
LIQUID
O
x

B

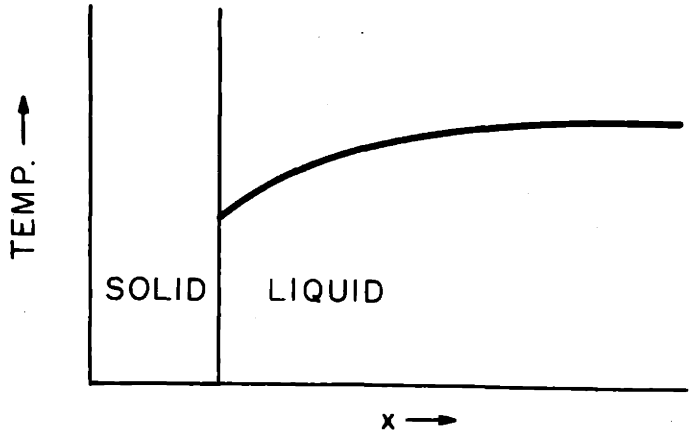
TEMP.
SOLID
LIQUID
x

C

Figure 2

Supercooling Resulting from the Actual Temperature Near the Surface Being Less Than the Liquidus Temperature.

a. Temperature Gradient in the Liquid.

b. No Temperature Gradient in the Liquid.

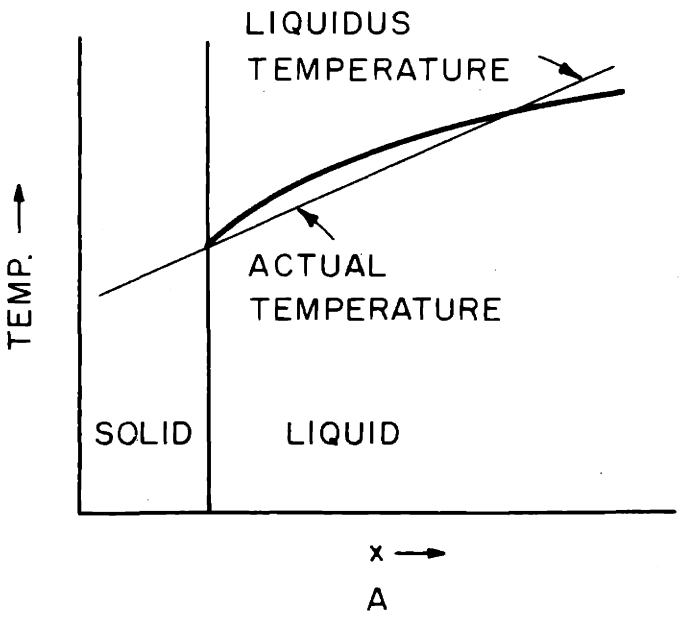
LIQUIDUS
TEMPERATURE
TEMP.
ACTUAL
TEMPERATURE
SOLID
LIQUID
x
A

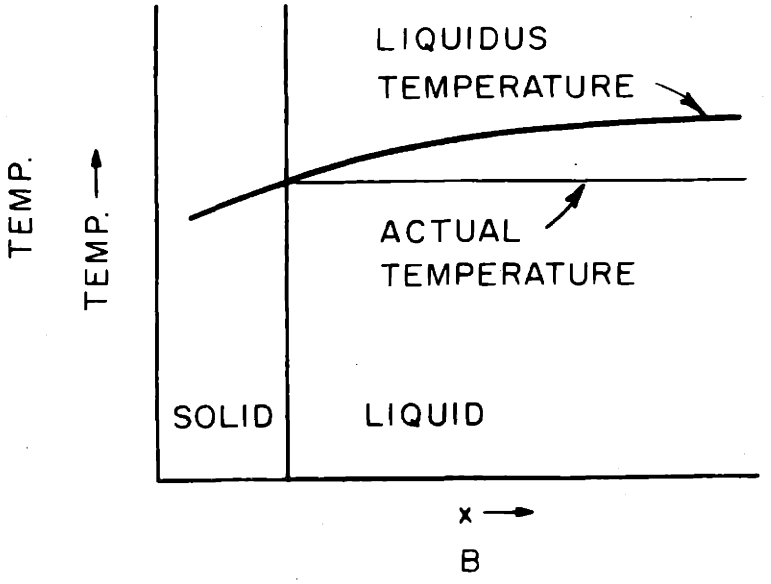
LIQUIDUS
TEMPERATURE
TEMP.
TEMP.
ACTUAL
TEMPERATURE
SOLID
LIQUID
x
B

Figure 3

Solute Concentration versus Distance for Dendrite Thickening Toward Mid-plane of Interdendritic Liquid.

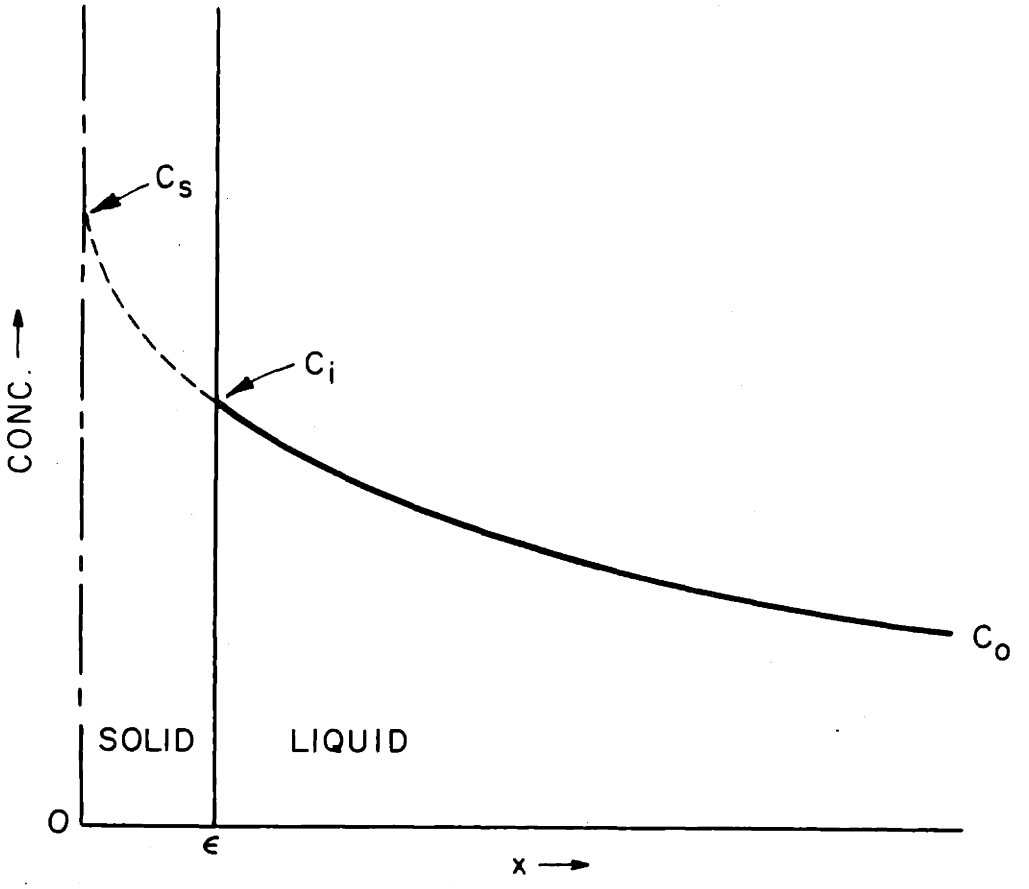
C_s
C_i
C_o
CONC.
SOLID
LIQUID
0
ϵ
x

Figure 4

D versus $\theta_f^{1/2}$, Plot of Equation (22).

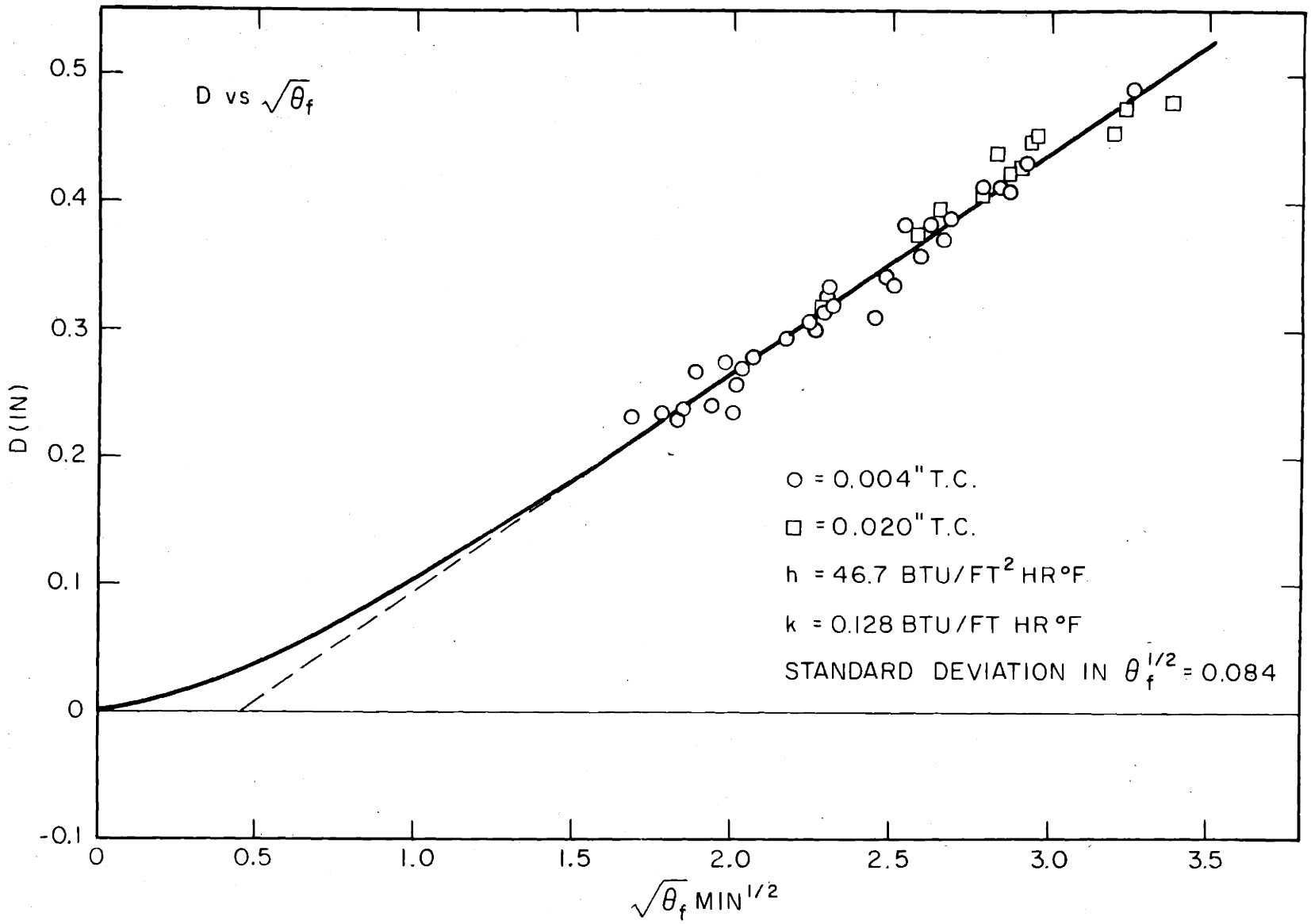
D vs $\sqrt{\theta_f}$
D (IN)
0.5
0.4
0.3
0.2
0.1
0
-0.1
0
0.5
1.0
1.5
2.0
2.5
3.0
3.5
$\sqrt{\theta_f}$ MIN$^{1/2}$
○ = 0.004" T.C.
□ = 0.020" T.C.
h = 46.7 BTU/FT^2 HR°F
k = 0.128 BTU/FT HR °F
STANDARD DEVIATION IN $\theta_f^{1/2}$ = 0.084

Figure 5

$\frac{\theta_f}{D}$ versus $\frac{1}{\frac{1}{D} + \frac{1}{\sqrt{\pi \alpha \theta_f}}}$, Plot of Equation (18).

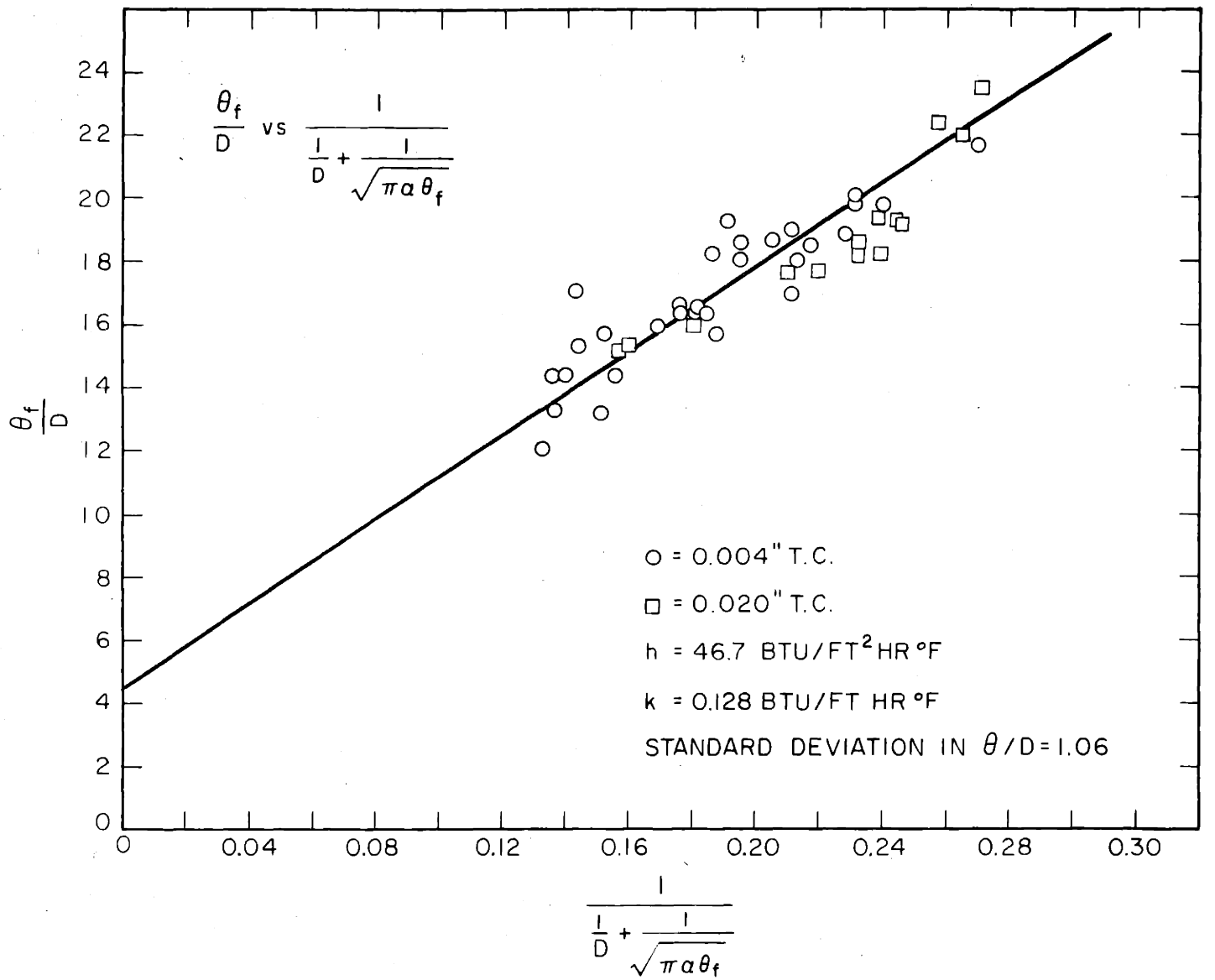
$\frac{\theta_f}{D}$ vs $\frac{1}{\frac{1}{D}+\frac{1}{\sqrt{\pi\alpha\theta_f}}}$
$\frac{\theta_f}{D}$
$\frac{1}{\frac{1}{D}+\frac{1}{\sqrt{\pi\alpha\theta_f}}}$
0
2
4
6
8
10
12
14
16
18
20
22
24
0
0.04
0.08
0.12
0.16
0.20
0.24
0.28
0.30
○ = 0.004" T.C.
□ = 0.020" T.C.
h = 46.7 BTU/FT^{2}HR °F
k = 0.128 BTU/FT HR °F
STANDARD DEVIATION IN θ/D = 1.06

Figure 6

A Reconstructed Time-Temperature Record Defining the Freezing Time as the Time Required for the Temperature to Fall 3°C.

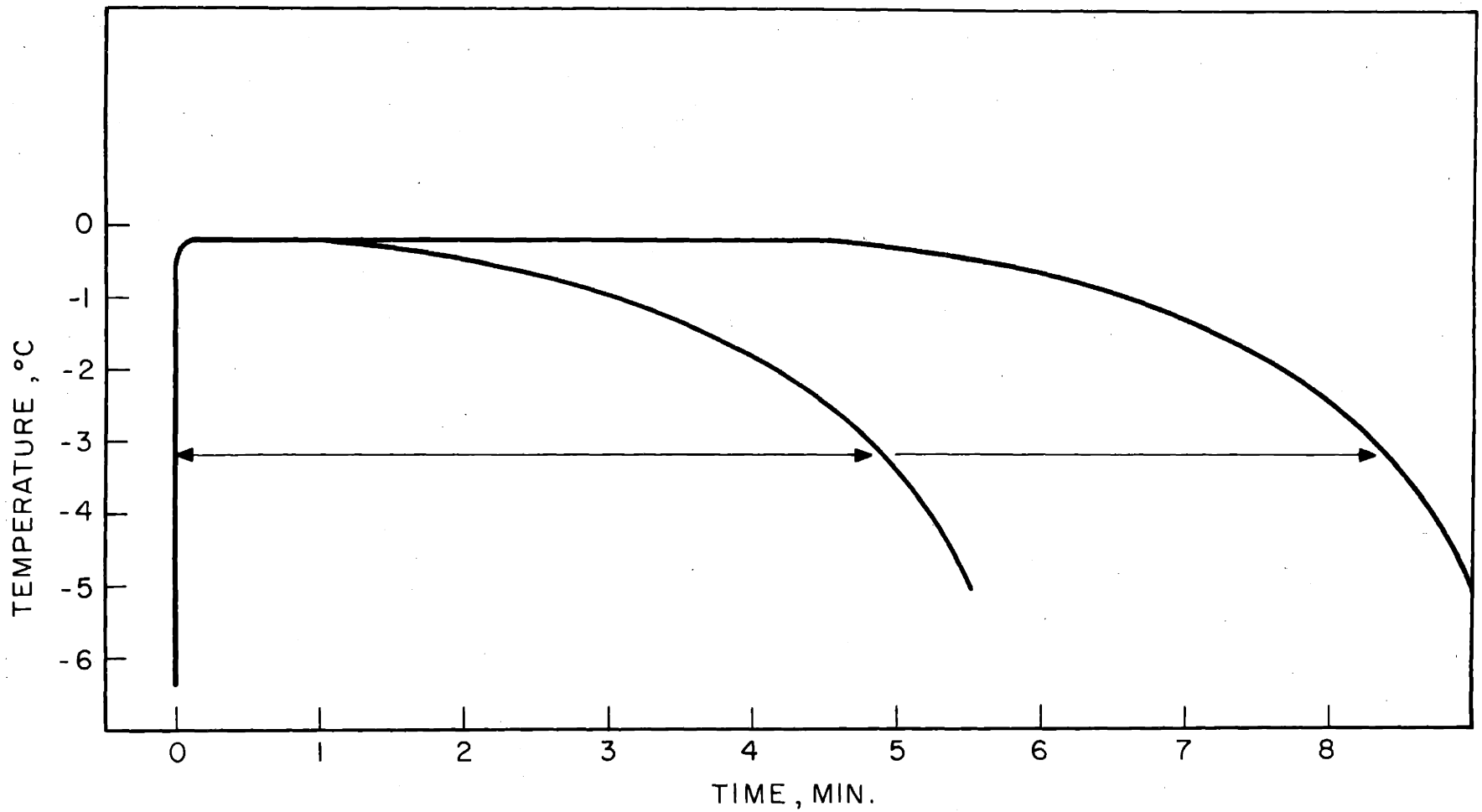

TIME vs TEMPERATURE DEFINITION OF θ_f

Figure 7

Photographs Showing the Platelet Nature of the Ice Dendrites (70 ×).

(a) is 90° to (c), and (b) is 45° to each.

A

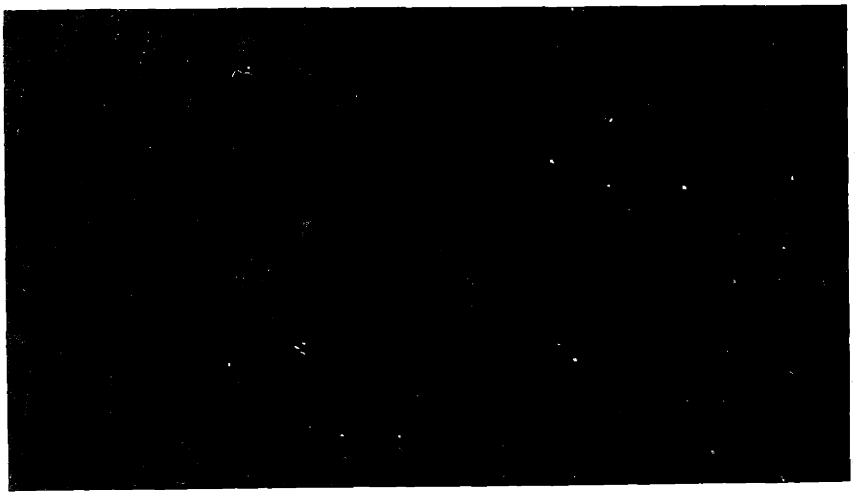

B

C

Figure 8

Distribution of Observed Dendrite Spacing.

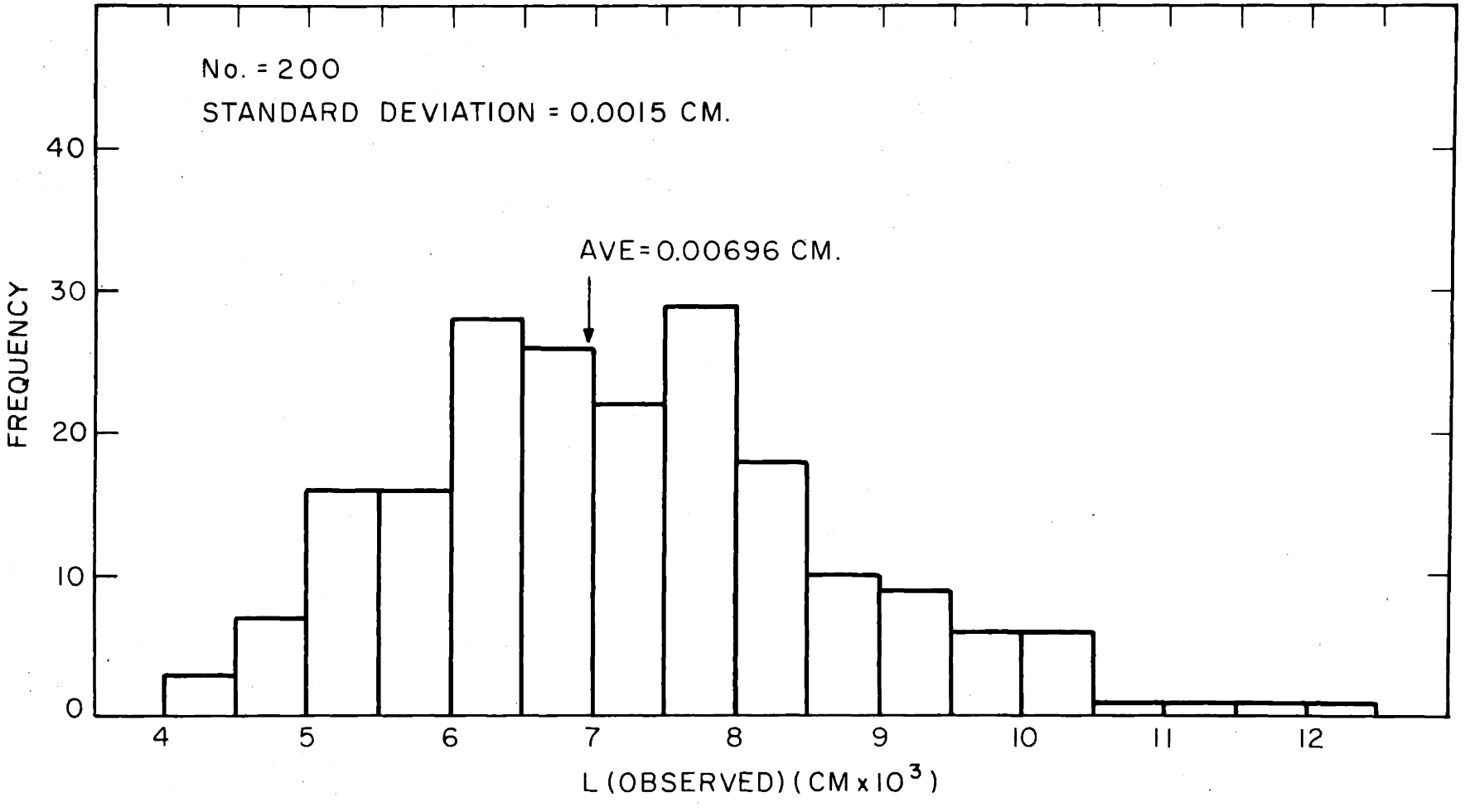

DISTRIBUTION OF OBSERVED DENDRITE SPACING

Figure 9.

Liquidus Temperatures for Sodium Chloride, Potassium Chloride, Lithium Chloride, and Hydrochloric Acid in the Region of Interest.

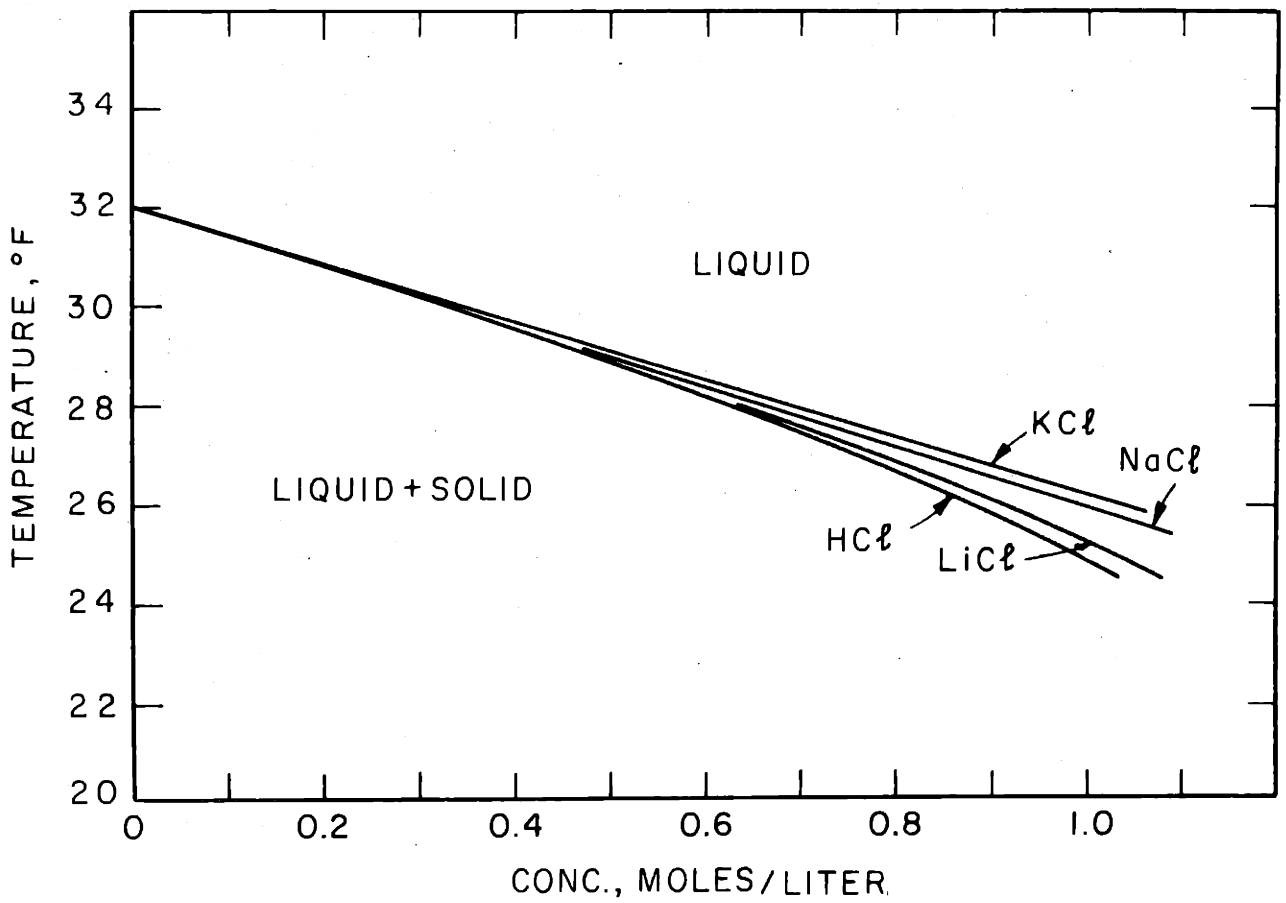

PHASE DIAGRAM OF KCℓ, NaCℓ, LiCℓ, HCℓ

Figure 10

Dendrite Spacing versus the Square Root of Freezing Time for Potassium Chloride Solutions.

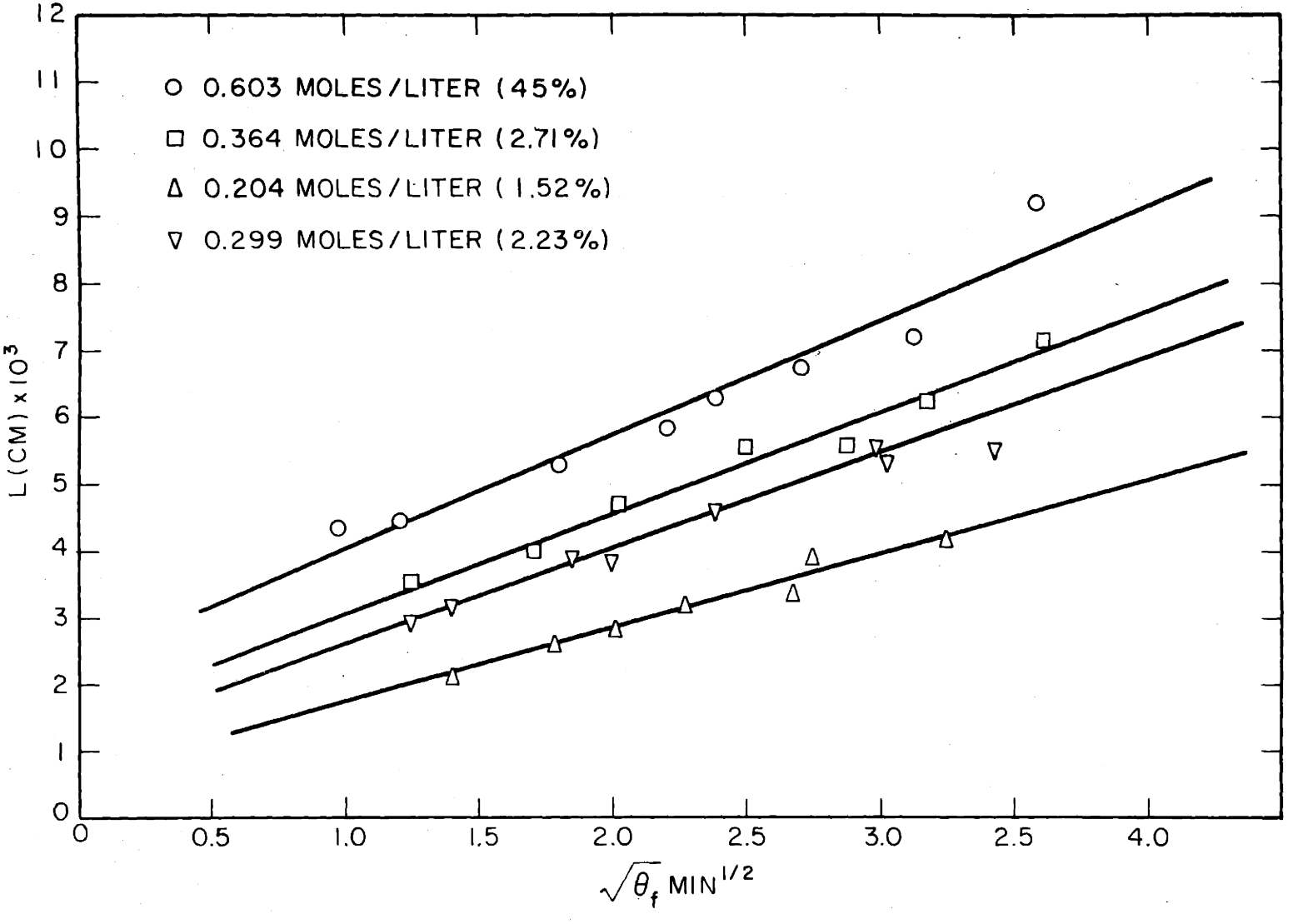

L vs $\theta_f^{1/2}$ FOR KCℓ

Figure 11

Dendrite Spacing versus the Square Root of Freezing Time for Potassium Chloride, Sodium Chloride, Lithium Chloride, and Hydrochloric Acid.

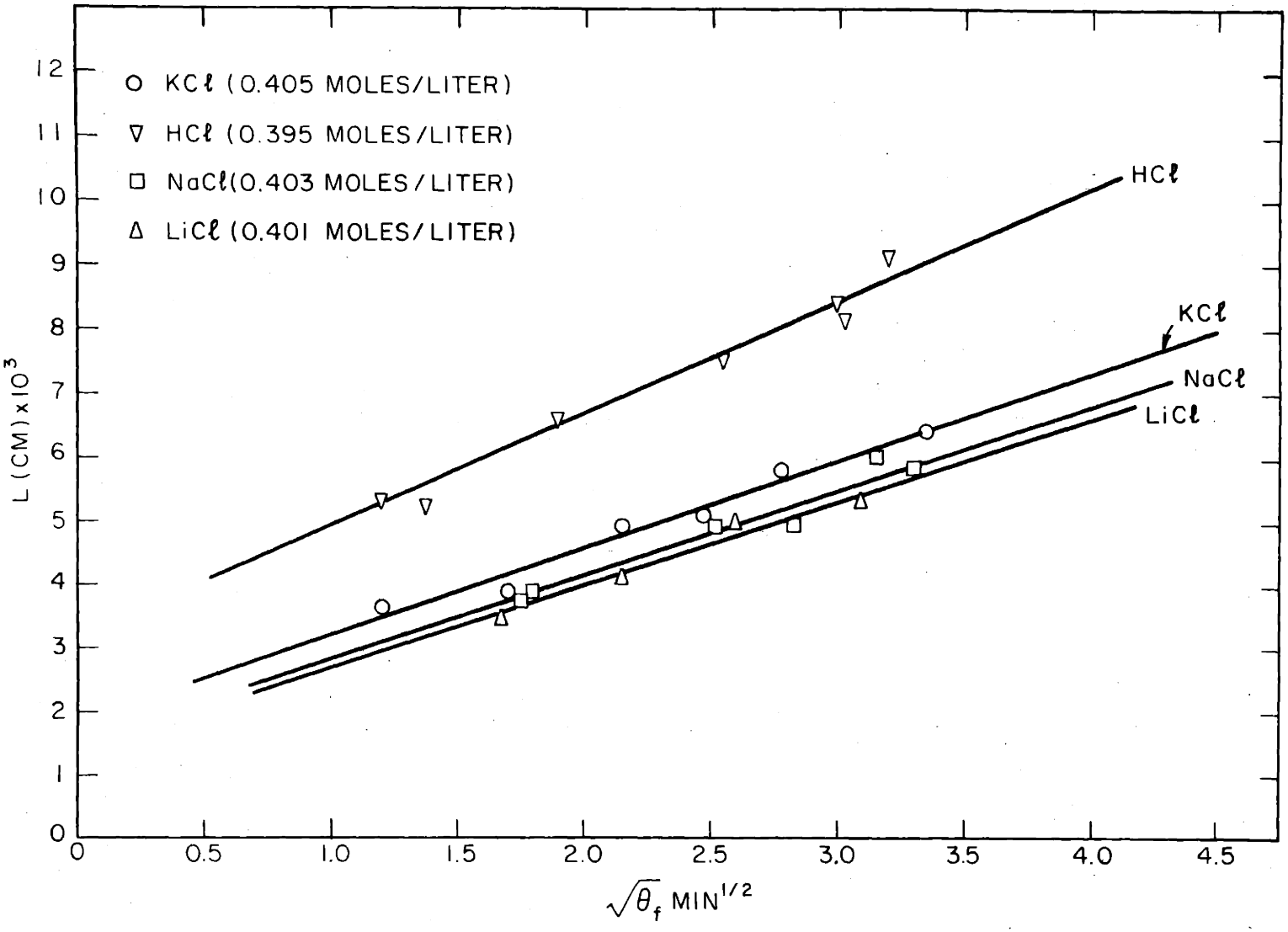

L vs $\theta_f^{1/2}$ FOR KCℓ, NaCℓ, LiCℓ, HCℓ

Figure 12

Supercooling Parameter, $\Delta T\sqrt{D'}$ versus Concentration of Potassium Chloride.

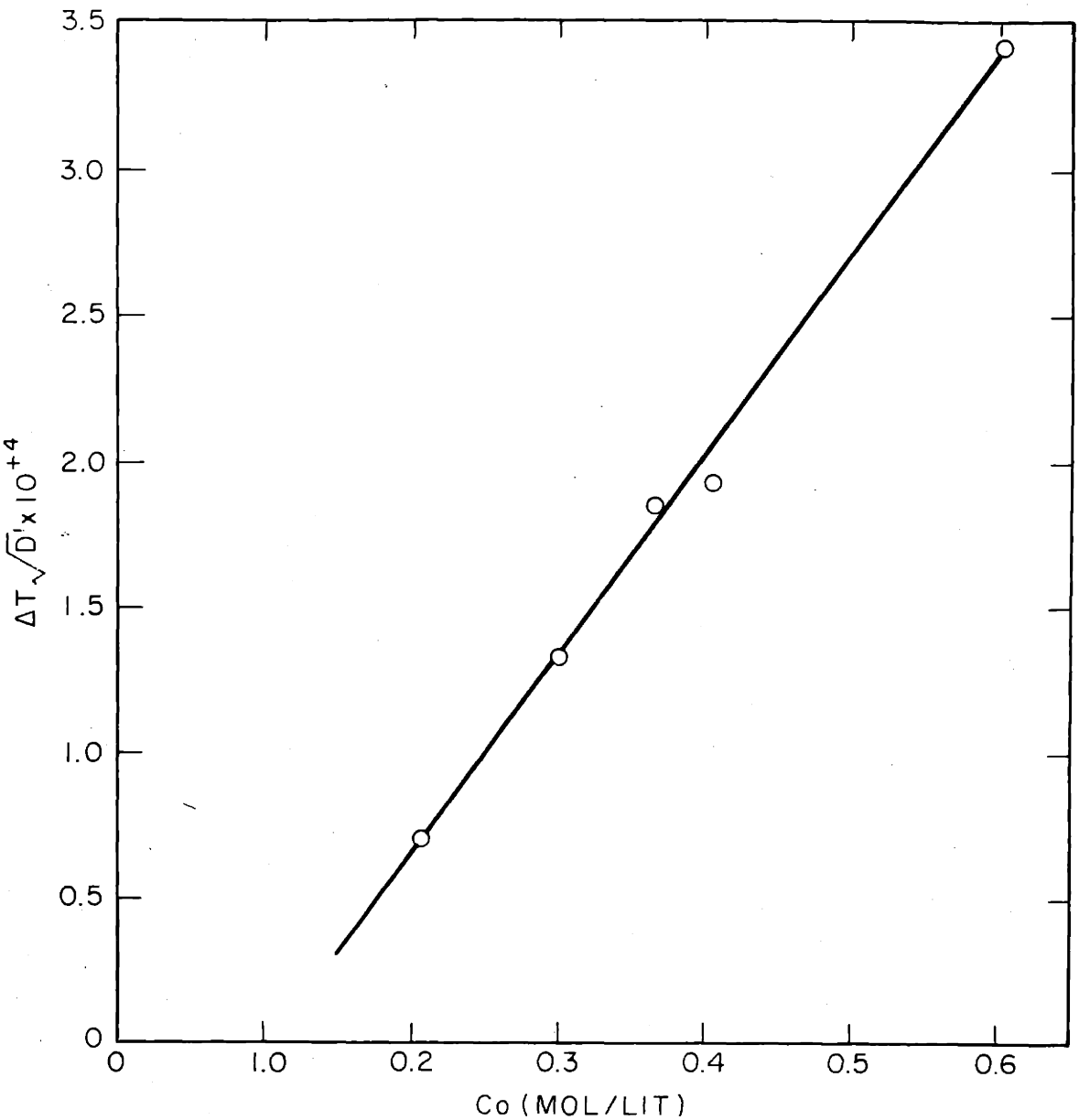

$\Delta T\sqrt{D'}$ vs Co FOR KCℓ

Figure 13

Comparison of Dendrite Spacing of Constant Composition but Different Freezing Times, 0.299 moles/liter KCl, 70 ×.

a. θ_f = 9.25 min.

b. θ_f = 2.19 min.

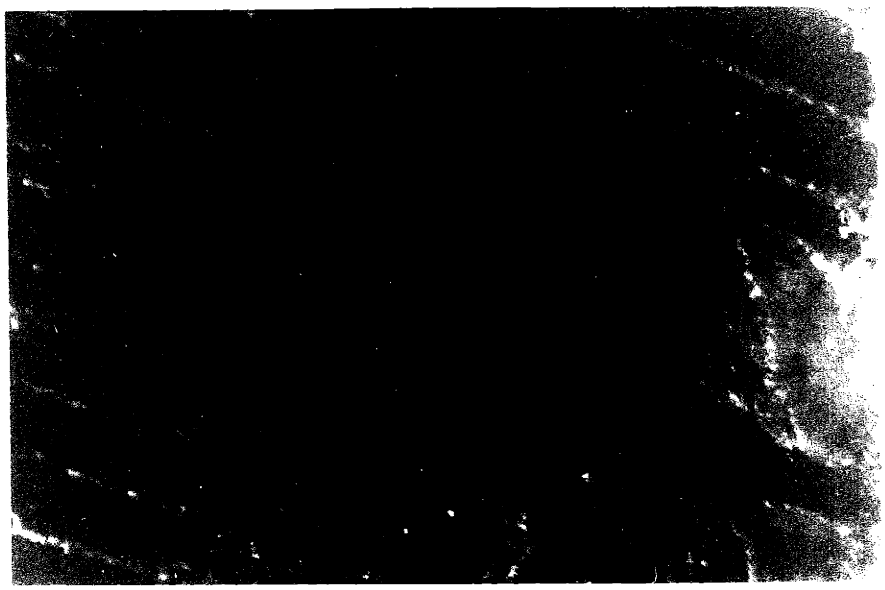

A

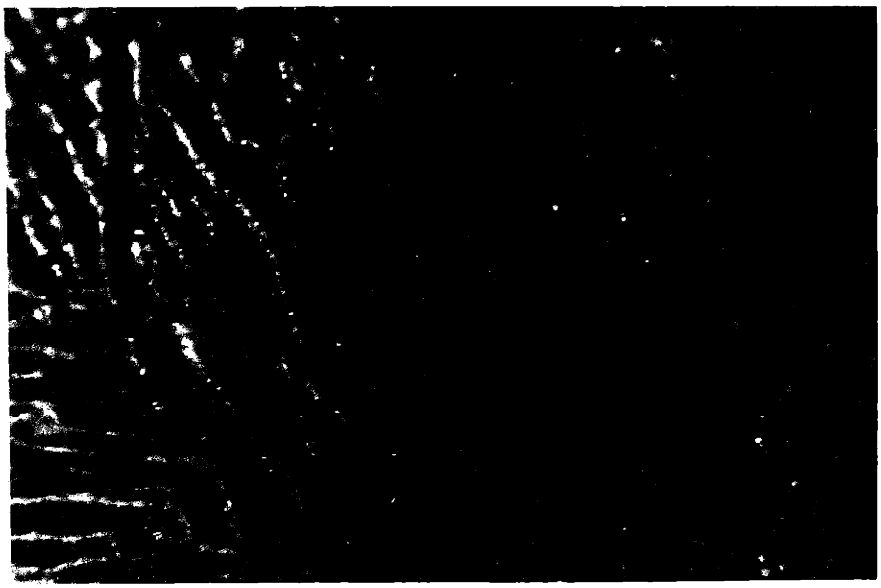

B

Figure 14

Comparison of Dendrite Spacing of Constant Composition and Freezing Time but Differing Diffusion Coefficients, 70 ×.

a. HCl, 0.395 mol/liter. θ_f = 9.15 min.

b. LiCl, 0.401 mol/liter. θ_f = 9.47 min.

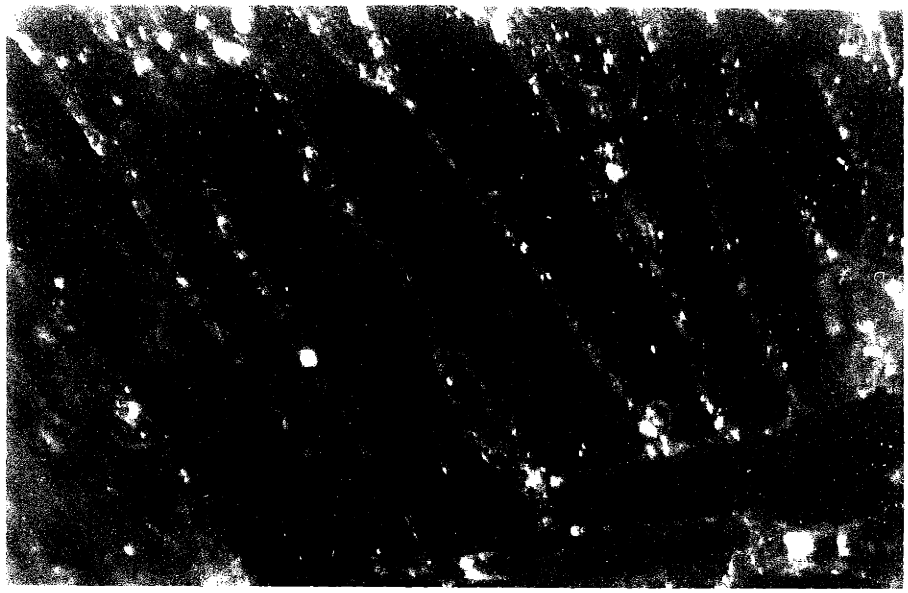

A

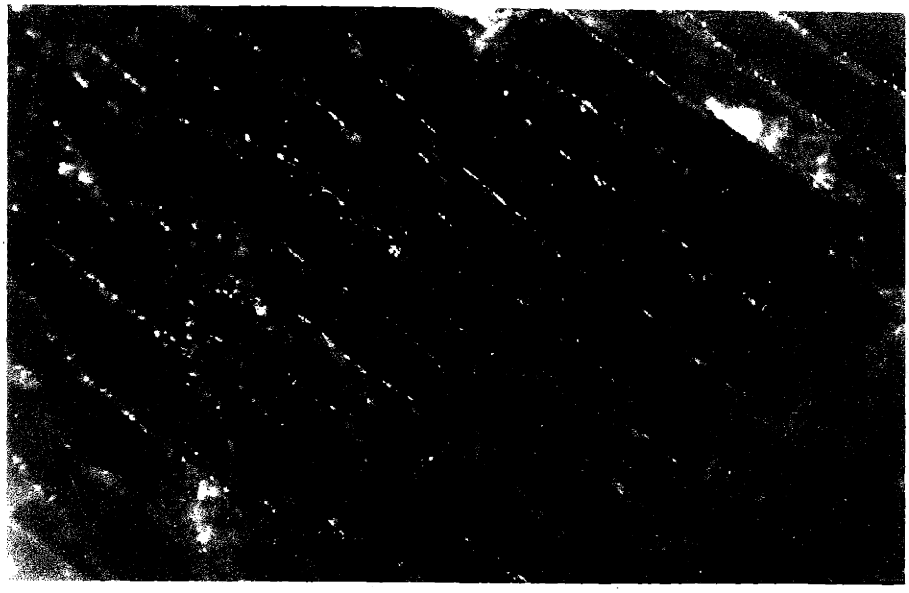

B

Figure 15

Comparison of Dendrite Spacing of Constant Freezing Times but Differing Concentrations of Potassium Chloride.

a. 0.603 mol/liter. θ_f = 5.29 min.

b. 0.204 mol/liter. θ_f = 5.20 min.

A

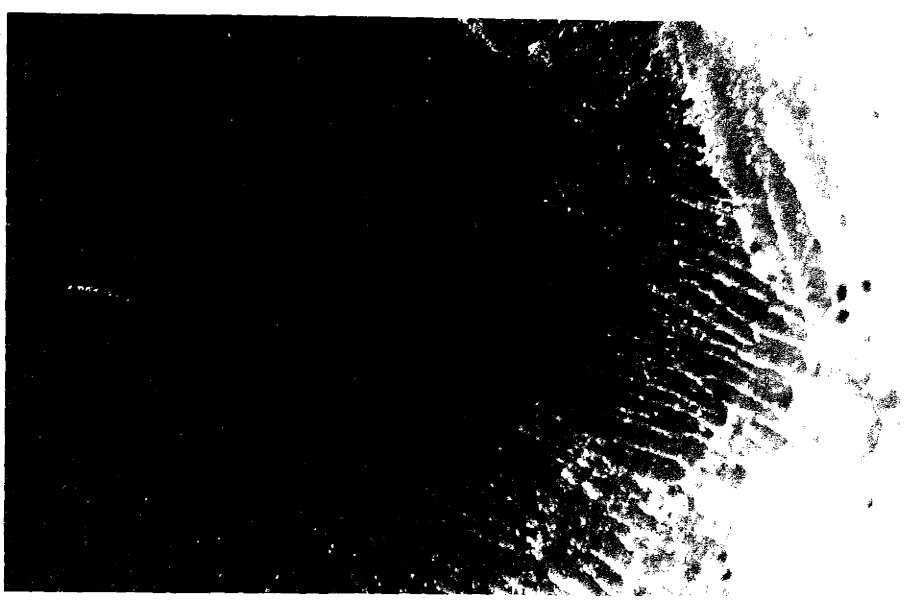

B

BIBLIOGRAPHY

1. Latimer, W. M., and J. H. Hildebrand, Reference Book of Inorganic Chemistry, Macmillan Co., New York (1951).

2. Morgan, J., and B. E. Warren, "X-Ray Analysis of the Structure of Water," Jour. Chem. Phys., 6, 666 (1938).

3. Bernal, J. D., and R. H. Fowler, "A Theory of Water and Ionic Solution, with Particular Reference to Hydrogen and Hydroxyl Ions," Jour. Chem. Phys., 1, 515 (1933).

4. Thompson, T. G., Physics of the Earth, National Research Council Bulletin 85, p. 63.

5. Frank, F. C., "Note on the Structure of a Crystal Surface," Phil. Mag., 41, 200 (1950).

6. Verma, A. R., "Observations on Carborundum Growth Spirals Originating from Screw Dislocations," Phil. Mag., 42, 1005 (1951).

7. Jackson, K. A., "Mechanism of Growth," Liquid Metals and Solidification, A.S.M., Cleveland (1958), p. 174.

8. Smith-Johannsen, R., "Some Experiments in the Freezing of Water," Science, 108, 652 (1948).

9. Chalmers, B., "Melting and Freezing," Trans. A.I.M.E., 200, 519 (1954).

10. Rutter, J. W., and B. Chalmers, "A Prismatic Substructure Formed During the Solidification of Metals," Canadian J. Phys., 31, 15 (1953).

11. Tiller, W. A., and J. W. Rutter, "The Effect of Growth Conditions upon the Solidification of a Binary Alloy," Canadian J. Phys., 34, 96 (1956).

12. Hucke, E. E., Flemings, M. C., Adams, C. M., and H. F. Taylor, "The Degeneration of Freezing Plane Interface in a Controlled Solidification System," Int. Symp. of Phys. Chem. of Proc. Met., A.I.M.E., Pittsburgh (1959).

13. Harrison, J. D., and W. A. Tiller, "Controlled Freezing of Water," in Proceedings of Endicott House Conference on Applied Glaciology, M.I.T. Press, in press.

14. Bolling, G. F., and W. A. Tiller, "Growth from the Melt. Part II. Cellular Interface Morphology," J. Appl. Phys., 31, 2040 (1960).

15. Brown, P. E., and C. M. Adams, "Structures Produced in Rapidly Solidified Alloys," Trans. A. F. S. (1962).

16. Himes, R. C., Miller, S. E., Mink, W. H., and H. L. Goering, "Zone Freezing in Demineralizing Saline Waters," Ind. and Eng. Chem., 51, 1345 (1959).

17. Weeks, W. F., "Tensile Strength of NaCl Ice," Jour. Glaciology, 4, No. 31, 25 (Mar. 1962).

18. Carslaw, H. S., and J. C. Jaeger, Conduction of Heat in Solids, Oxford (1947).

19. Adams, C. M., "Thermal Considerations in Freezing," Liquid Metals and Solidification, A.S.M., Cleveland (1958), p. 187.

20. International Critical Tables, 4, 254 (1933). Published for the National Research Council by McGraw-Hill Book Co., Inc., New York.

21. Robinson, R. A., and R. H. Stokes, Electrolyte Solutions, Academic Press, Inc., New York (1955).

22. Newman, F. H., Electrolyte Conduction, John Wiley and Sons, New York (1931).

23. Hamilton, L. F., and S. G. Simpson, Quantitative Chemical Analysis, Macmillan Co., New York (1955).

BIOGRAPHICAL NOTE

The author was born in Newton, Massachusetts, on January 24, 1936. After graduating from Newton High School in 1954, he entered M.I.T., from which he received his S.B. in 1958 and S.M. in 1959. Since 1959 he has been a Research Assistant in the Department of Metallurgy. He has participated for a portion of this period in a sea ice study at Point Barrow, Alaska, Eglin Air Force Base, Florida, and Thule, Greenland, under the sponsorship of the Air Force Cambridge Research Laboratory.

He is a member of the Society of Sigma Xi, American Institute of Metallurgical Engineers, American Society for Metals, and the British Glaciological Society.

He has been married to the former Louise A. Murray since June, 1960, and has one daughter, Katherine Louise.